AD-A195 894 ACTA AERONAUTICA ET ASTRONAUTICA SINICA (SELECTED ARTICLES)(U) FOREIGN TECHNOLOGY DIV WRIGHT-PATTERSON AFB OH 10 FEB 88 FTD-ID(RS)T-1193-87 1/1

UNCLASSIFIED F/G 1/2 NL

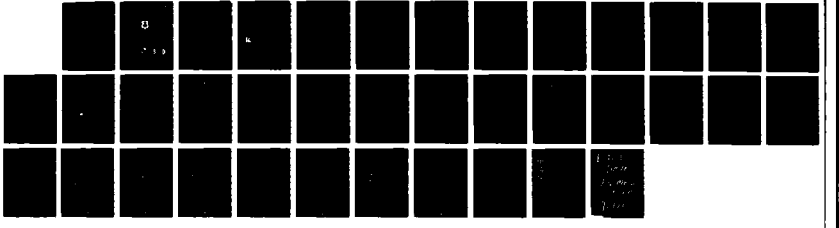

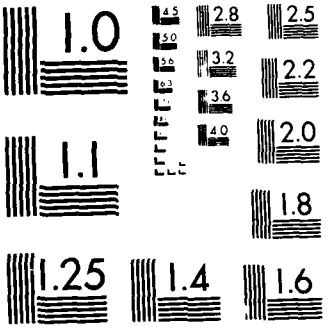

FTD-ID(RS)T-1193-87

DTIC FILE COPY

FOREIGN TECHNOLOGY DIVISION

ACTA AERONAUTICA ET ASTRONAUTICA SINICA

(Selected Articles)

Approved for public release;
Distribution unlimited.

88

HUMAN TRANSLATION

FTD-ID(RS)T-1193-87 18 February 1988

MICROFICHE NR: FTD-88-C-000394L

ACTA AERONAUTICA ET ASTRONAUTICA SINICA
(Selected Articles)

English pages: 31

Source: Hangkong Xuebao, Vol. 8, Nr. 2,
February 1987, pp. 1-10; 11-18

Country of origin: China
Translated by: FLS, INC.
F33657-85-D-2079
Requester: FTD/TQTA

PREPARED BY:

TRANSLATION DIVISION
FOREIGN TECHNOLOGY DIVISION
WPAFB, OHIO.

TABLE OF CONTENTS

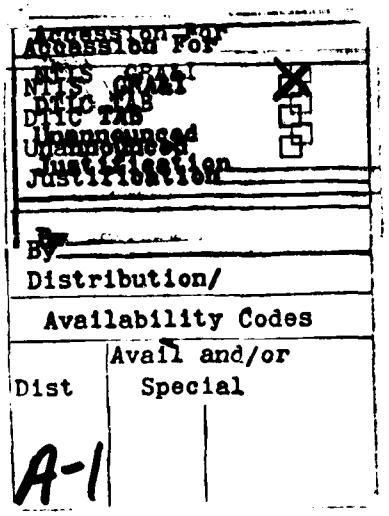

GRAPHICS DISCLAIMER

All figures, graphics, tables, equations, etc. merged into this translation were extracted from the best quality copy available.

New Content of Tactical-Technical Requirements for Military Aircrafts in the Early Part of the 21st Century---the Stealth Penetration Ability

Zhang Kao

Beijing institute of Aeronautics and Astronautics

Submitted December 16, 1986

Abstract

This paper demonstrates the importance of stealth penetration ability for future military aircrafts via three areas such as the inspirations from war, the conclusions of a system engineering analysis and the threats from anti-stealth techniques, etc. The emphasis of this paper is placed on the analysis of the new content of tactical-technical requirements for military aircrafts in the early part of the 21st century---the three categories included in the stealth penetration ability are: (1) scattering and radiation characteristics of aircrafts; (2) electronic interference ability of aircrafts; (3) tactical stealth techniques used by aircrafts.

I. Importance of Stealth Penetration Ability of Aircrafts

The stealth aircrafts have been deployed in military services in foreign countries, and their advent has an epoch-making significance which will force the existing air defense systems into making fundamental changes; whereas new air defense systems in turn will force the stealth aircrafts to develop toward still higher levels. It is predicted that the early part of the 21st century is the era when the new air defense systems will begin to emerge and, it may be said that, by that time, aircrafts without stealth penetration ability are extremely vulnerable.

1. Inspirations from war

Several local wars fought after the Second World War have made people recognize more and more the important effects of electronic defense techniques in modern warfares. During the fourth Middle East War in 1973, the Israelis suffered heavy losses under the attack of Egyptian SA-6 guided missiles and anti-aircraft guns with radar-commanded sights, since their aircrafts did not use any electronic defense techniques. Later, the Israelis bought radar interference devices from the U.S. and installed them on some of their aircraft, and very few of these aircfrafts have been shot down ever since. The Israelis have learned a lesson from past wars and utilized various advance equipment to have skillfully waged a successful electronic war during the Middle East War in 1982, and the Syrian air defense systems were totally demolished after a very short period of combat. Among which the mini-type, remote-controlled stealth aircrafts built by the Israelis has broght outstanding effects into play.

The armed helicopters used by the U.S. Air Force in the battlefields of Vietnam had been repeatedly shot down by the Russian-made SA-7 infrared seeking guided missiles to have caused tremendous losses. Infrared suppression devices were installed on armed helicopters later on, and consequently the probability of their being hit by SA-7 had been effectively reduced.

Experience from wars has shown people that, in the face of various effective and sensitive searching, tracking and sighting devices, without any stealth penetration ability the aircraft's survival ability is seriously threatened. Conversely, as long as a certain or several stealth counter measures are taken their survival ability will be markedly increased.

2. System engineering analysis

Figure 1 is the results of a system engineering analysis for the relations between survival ability and stealth technique conducted by a certain American company. Curve (1) in the figure is the un-reduced radar scattering cross-section, without using any anti-electronic devices; curve (2) is the reduced radar scattering cross-section without using any anti-electronic devices; curve (3) is the reduced radar scattering cross-section with anti-electronic devices. This analysis has convincingly illustrated the influence of stealth penetration ability on the

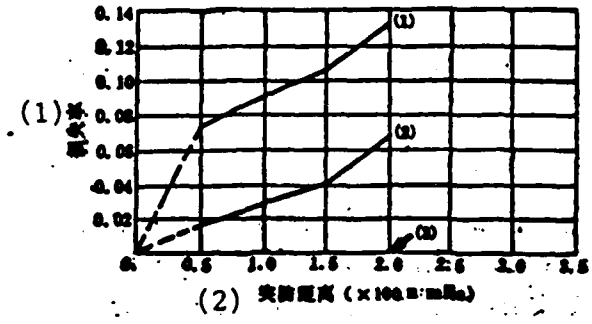

Fig. 1 Relations between stealth penetration ability and survival ability.
Key: (1) Loss rate; (2) Penetration distance (×100 n mile)

survival ability. If the radar scattering cross-section reduction technique is combined with anti-electronic technique and applied to one airplane, then this airplane is capable of obtaining safe penetration of a defense line throughout the entire flight.

3. Threats from anti-stealth techniques

Just like stealth techniques, the anti-stealth techniques also come in all different types. Take the radar wave anti-stealth technique for example, it is currently taking on various areas such as new radar systems and new test theories in the domains of air, frequency, time and polarization to expand the amount of signals to be tested and raise the sensitivity and anti-interference ability, etc. It may be predicted that, after another 10-15 years of development in anti-stealth techniques, the new generation of radar may very possibly make the first generation stealth aircrafts lose their stealth penetration ability. By that time, there will be a leap in the quality of microwave detection, infrared detection and various acoustic and optical remote-sensing detection system. It is only natural that the struggle between stealth and anti-stealth techniques will be carried on one generation after another. Just as scholars and experts in foreign countries have pointed out that: before the 80's, the aircraft designer's efforts had always been steered toward the direction of continuous perfection in aerodynamics and continuous increase in structural efficiency; whereas a new direction requiring efforts has been added after the 80's: the continuous decrease in aircraft radar scattering cross-section. Therefore, faced with constant increase in the detection ability of various remote-sensing detection systems, if the aircraft designers do not try to increase the aircraft's stealth penetration ability by summoning all available techniques, the survival ability of aircraft will be severely damaged.

II. The Primary Contents and Measures of the Stealth Techniques

The contents of the stealth techniques primarily include the following four categories:

1. Infrared-ray stealth techniques: (1) blocking radiation source; (2) adding additives in fuel to change the infrared frequency band; (3) injecting infrared absorbent into the exhaust flames; (4) installing infrared suppression device at the jet nozzles; (5) adopting twin-nozzle; (6) employing infrared interference devices.

2. Radar wave stealth techniques: (1) technique for reducing radar scattering cross-section: (a) contour technique; (b) material technique; (c) resistance-bearing technique; (d) low scattering cross-section on-board radar antenna technique; (2) electronic interference techniques (with source, without source and radar bait); (3) tactical stealth techniques.

3. Visible light stealth techniques.

4. Sound wave stealth techniques.

Since the threats to existing military aircrafts primarily come from radar detection devices and infrared detection devices, consequently the present research in stealth techniques in foreign countries mainly concentrates on the first two categories. The investment in radar wave stealth techniques by the U.S. has exceeded 30 billion dollars, and the investment in long-range stealth bomber ATB alone has exceeded 7.5 billion dollars with more than 5,000 technical personnel assembled for man power.

For visible light stealth techniques, the ancient but effective simulated background camouflage coating method is still in used. The new scope for research is to make the brightness of coating changes automatically with the brightness of background.

The primary content of sound wave stealth techniques is to build super-low noise power equipment, and the U.S. has already entered the functional stage.

For infrared-ray stealth techniques, adopting the twin-nozzle is a very effective measure. It can decrease the intensity of source radiation directly behind the nozzles by 90% (see Fig. 2 and Fig. 3). It can also be seen from Fig. 3 that the device tracking range of twin-nozzle under infrared seeking decreases markedly compared to that of the axially symmetrical nozzle. The U.S attack aircraft A-10 (see Fig.4) adopted the aerodynamic configurations of back-carrying engines. This kind of aerodynamic configurations can effectively reduce the infrared tracking range, drawing support from blockage of flame radiation by fuselage, horizontal and vertical tail fins. The U.S. high-altitude unmanned aircraft AQM-34N(H) had been using the flame infrared absorbent. The infrared suppression device mentioned earlier has currently become the standard component for the U.S armed helicopter. The U.S. has installed infrared interference devices (including infrared bait) on F-4 and some of the other military aircrafts.

For radar wave stealth techniques, the theoretical research in resistance-bearing technique in foreign countries has been conducted for a longer period; currently, however, there has not been any report on its actual application, possibly due to security reason. The On-board radar antenna is a strong scattering source and the problem of either reducing or shielding this scattering source has become a very important subject with a high degree of difficulty.

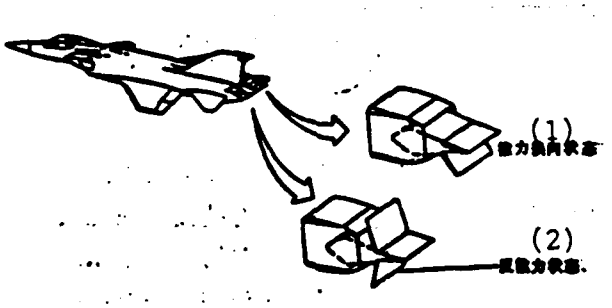

Fig. 2 Double-throat type twin-nozzle
Key: (1) Propulsion in direction-changing state;
(2) Counter-propulsion state

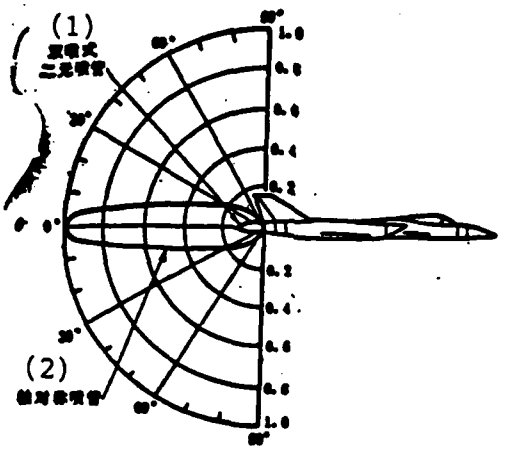

Fig. 3 Infrared Radiation Characteristics of the double-throat type twin-nozzle
Key: (1) Double-throat type twin-nozzle; (2) Axially symmetrical nozzle.

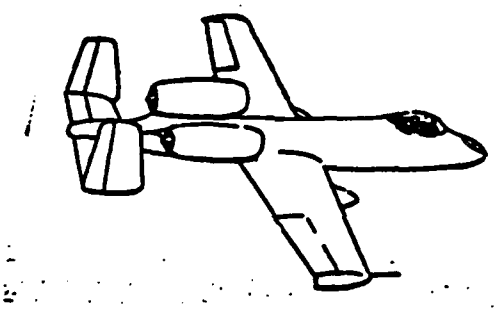

Fig. 4 A-10 attack aircraft

The primary contents (or measures) of contour technique for reducing radar wave scattering cross-section can be summarized as follows: eliminate contour combination which causes the generation of angular reflector effect; change backward scattering to non-backward scattering; subsititute mirror reflection with peripheral diffraction; substitute curved contour with flat contour; decrease number of scattering sources; reduce the size of aircraft; and use a certain component to block another component, etc. Refer to Reference [11] for the associated measures and applications described above. The contour technique possesses a great potential. It can reduce, under the premise of not obtaining significant breakthrough in aerodynamics and power equipment, the radar scattering cross-section of military aircrafts by 75-90%; whereas under the premise of obtaining significant breakthrough in aerodynamics and power equipment, it can reduce the radar scattering cross-section by 90-99%. Combining contour technique with material technique and

material technique and on-board antenna technique can reduce the radar scattering cross-section of military aircrafts by 99-99.9% or even more.

Material technique may not be interpreted as consisting only of the manufacturing of high performance microwave absorbing material; rather, among which the research in material applications (including wave-absorption and wave-transparent, electrically conductive material) also occupies an important position. People often ignore such a fact: for some components or sections, combining contour technique and using electrically conductive material can reduce more radar scattering cross-section than using wave-transparent or wave-absorption material. The study of material application is exactly for solving problems such as at what section, combining with what contours and using what material will enable the aircraft to effectively reduce its radar scattering cross-section. The example in Fig.5 convincingly proves the above point. The structural type wave-absorption material has been successfully applied on stealth aircraft in foreign country. Local application of coat-cover type wave-absorption material (coating adhesive film) on stealth aircraft in foreign countries has already displayed its unique advantage, but large area application has not been realized. Mainly because this kind of material still has serious shortcomings such as large specific gravity; coating layer too thick; and working freguency band not wide enough, etc. But it is being rapidly improved.

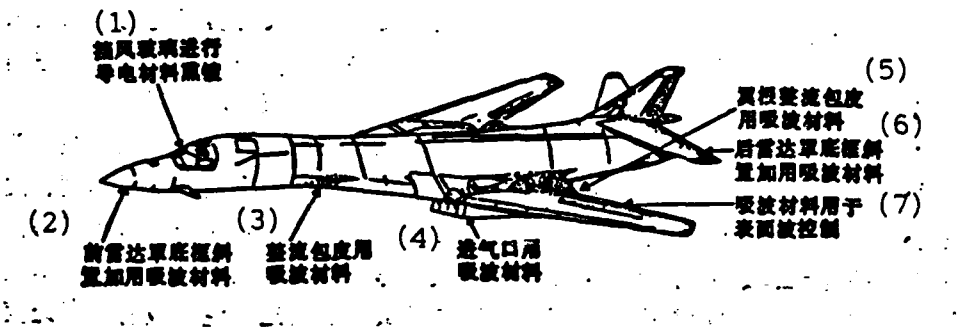

Fig. 5 Application of material technique on B-1B bomber
Key: (1) Wind shield undergoes fumigation-plating with electricallly conductive material; (2) Bottom frame of the front radar dome is tilt-mounted with wave-absorption material added; (3) Flow-regulating wrapper uses wave-absorption material; (4) Air-intake uses wave-absorption material; (5) Flow-regulating wrapper at wing root uses wave-absorption material; (6) Bottom frame of the rear radar dome is tilt-mounted with wave-absorption material added; (7) Wave-absorption material is used for surface wave control.

Electronic interference technique has been successfully employed for several decades; however, the radar scattering cross-section of aircraft itself must be markedly reduced in order for this technique to bring its effects into play more effectively.

Tactical stealth techniques include many contents, but its basic implication is to draw support from a set of electronic device to control the flight path of an aircraft in order to evade the effective detection direction of radar antenna or make its weaker scattering direction aim at the radar antenna. Since a set of perfect electronic device is the key to assuring tactical stealth penetration, the tactical stealth penetration, therefore, may also be summed up into the confrontation of electronic techniques.

There are strong and weak points in any kind of stealth penetration technique. Only by organically combining various techniques---propagating the strong ones while discarding the weak ones to make one technique the effective utilizing and creating condition of another technique, can high performance stealth aircrafts be manufactured.

III. Contents and Indexes for Expressing Stealth Penetration Ability in Tactical Technique Requirements

The remote-sensing detection systems currently faced by aircraft mainly come in four categories, i.e. radar detection system; infrared detection system; optical detection system and acoustic detection system. Judged by their development, the contents of these four categories will be gradually enriched and their implications will also be drastically changed with detection systems combining two or several theories starting to appear. The so-called "stealth penetration ability" means the ability of an aircraft to conceal its flight under the operation of various remote-sensing systems described above. Currently or during a period from today, the stealth penetration ability in the tactical technique requirements will mainly (or at least) include the ability to conceal flight against the former two detection systems.

The stealth penetration ability can be materialized through the following contents in three categories:

1. Scattering characteristics and radiation characteristics of aircraft

(1) Electromagnetic scattering characteristics of aircraft. For radars, we call the intensity of electromagnetic scattering generated along the direction of radar reception antenna by aircraft under the irradiation of radar wave the "radar scattering cross-section", and its unit is m^2 or dBm^2 [8]. The numerical value of the radar scattering cross-section of an aircraft displayed in different radar irradiation directions (or called the angle of posture, i.e. the angles ϕ and θ in Fig. 6) change drastically. Fig. 7 is the electronmagnetic scattering characteristic curves plotted using the average value taken from the drastically changing radar scattering cross-sections within a range of every 5 degrees. Other than irradiation direction, the magnitude of radar scattering cross-section is also determined by the contour, size and structure of the aircraft as well as the wavelength and polarization pattern of the radar wave[8]. If we calculate or test the curves of radar scattering cross-section which change with the angle of direction ϕ and angle of pitch θ corresponding to several primary wavelengths and polarization patterns discussed which may be encountered by an aircraft, then the electromagnetic scattering characteristics of this aircraft are thus fully expressed. This is one of the tactical technique indexes which a new aircraft should possess when undergoing scheme evaluations. However, these steps can not be carried out before the design drawings are completed. Therefore, only the numerical values of radar scattering cross-section on a few critical angles of posture in the tactical technique requirements proposed for an aircraft which is about to be designed need to be limited. And yet these numerical values of radar scattering cross-section must correspond to the radar types (operating systems, wavelength and polarization pattern) that may be encountered by the said aircraft. For example, long-distance penetration is not considered for a short-range fighter; rather, the main consideration is the threats from on-board or on-missile radar during air combat conditions. Therefore, it is required to first predict the operating systems (single-station or multi-station, with or without downward vision, etc.) of this kind of radar on the enemy's side, then determine to what degree must the radar scattering cross-section be limited within what range of angle of posture. Another example, except for considering the enemy's radars encountered during air combat for a long-range bomber, factors such as long-range warning radar, guidance radar, and gun-sight radar, etc. that may be encountered during long-distance penetration process must also be considered. The primary range of angle of posture to which attention must be paid and the degree to which radar scattering cross-section must be limited are determined based on these subjects.

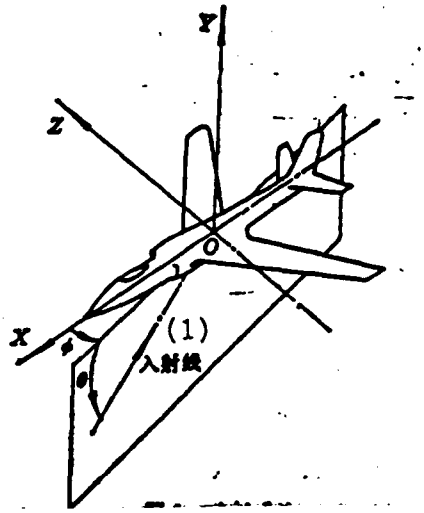

Fig. 6 Coordinate system.
Key: (1) Incident ray.

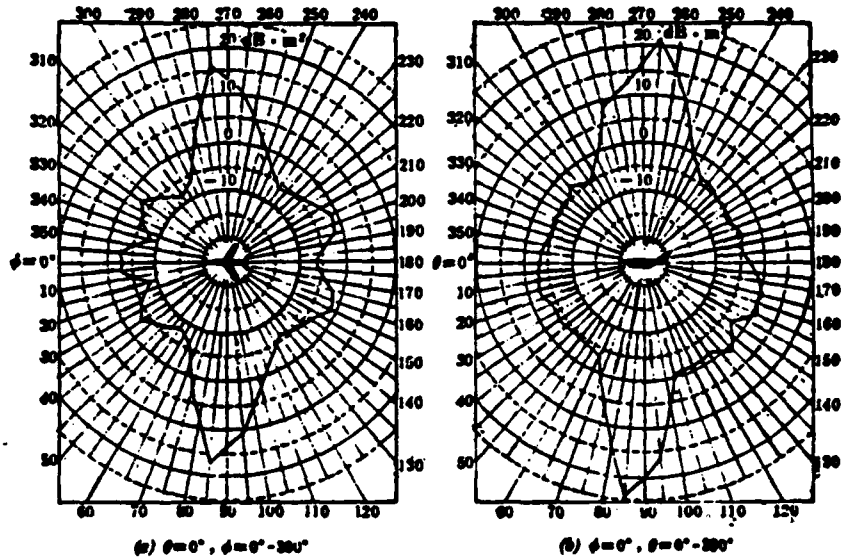

Fig. 7 Electromagnetic scattering characteristics of an unmanned aircraft (x wave section, horizontal polarization)

Table 1 lists the radar cross-sections of various types of aircraft under direct front irradiation. It may be seen that, for the same type of aircraft, the scattering cross-section of a stealth long-range bomber ATB is only one-thousandth of that of a regular long-range bomber B-52. Data in Table 2 is based on the level demonstrated in foreign countries and the results obtained from studies of potential analysis.

Table 1 Direct front radar scattering cross-section σ

(1)飞行器名称	(3)B-52	(4)B-1A	(5)B-1B	(6)ATB	(7)F-16	(8)AQM-34N(N)	(9)飞鱼
(2)类型	远程轰炸机	远程轰炸机	远程轰炸机	远程轰炸机	战斗机	无人驾驶战略侦察机	反舰导弹 (10)
σ(m²)	100	10	1	<0.1	1~2	0.5	0.1

Key: (1) Name of Aircraft; (2) Type; (3) Long-range bomber; (4) Same as (3); (5) Same as (3); (6) Same as (3); (7) Fighter; (8) Unmanned strategic reconnaissance drone; (9) Exocet; (10) Anti-ship guided missile.

Table 2 Predicted direct front radar scattering cross-section σ for military aircrafts in the early part of the 21st century

表2 (2) (3) 推测21世纪初军用飞行器正前方的雷达散射截面σ (7)

(1)飞行器类型	远程轰炸机	战斗机	(4)无人战略侦察机	(5)无人战术侦察机	(6)巡航导弹	反舰或空地导弹
σ(m²)	0.05~0.1	0.01~0.05	0.005~0.01	0.001~0.005	0.005~0.01	0.001~0.01

Key: Type of Aircraft; (2) Long-range bomber; (3) Fighter; (4) Unmanned strategic reconnaissance drone;(5) Unmanned tactical reconnaossance drone;(6) Cruise missile; (7) Anti-ship or air-to-surface guided missile.

(2) Infrared radiation characteristics of aircrafts

The engine exhaust flame is the main infrared radiation source of an aircraft. For infrared detection system, one of the aspects of stealth penetration ability of an aircraft within the tactical technique requirements can be expressed as the intensity of infrared radiation around the engine exhaust flame along the reception direction of the infrared seeking device. Its implication is the infrared radiation power within an unit solid angle and its dimention is watt/solid radian. Fig. 8 shows the infrared radiation characteristics within a horizontal plane. Generally, the infrared radiation characteristic curves behind an aircraft are not symmetrical to the aircraft axis and therefore, the infrared characteristic curves within a vertical plane are still required.

Certain parts of the structural surface of some of the transonic and supersonic aircrafts also constitute the tracked radiation sources for infrared seeking devices due to aerodynamic heating, and the infrared radiation characteristic curves for this kind of sources should also be given.

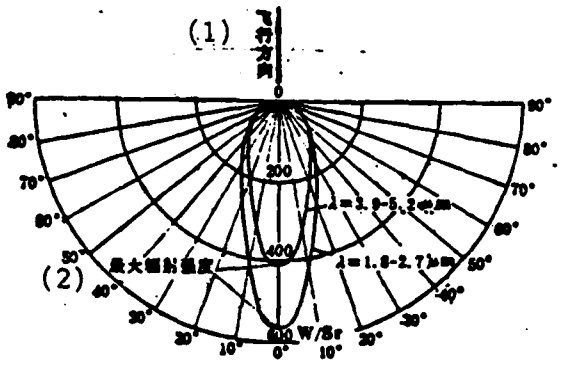

Fig. 8 Infrared radiation characteristics of a certain jet plane
Key: (1) Flight direction; (2) Maximum radiation intensity.

A complete set of infrared radiation characteristic curves are one of the indispensable tactical technique indexes for scheme evaluation of a new aircraft. In the tactical technique requirements proposed before starting the design of a new aircraft, at least the maximum intensity of infrared radiation not exceeding how many W/sr in several critical directions of the aircraft (these directions must predict the attackable directions of a target by infrared seeking weapons when the new aircraft is deployed) and in several wave sections sensitive to infrared seeking devices must be clearly specified.

2. Electronic interference ability

Just by reducing the radar scattering cross-section of an aircraft can not really guarantee the aircraft's not being discovered under all conditions, especially when the aircraft is very close to the radar. At such time, the aircraft's anti-detection and anti-tracking must still draw support from electronic interference devices or tactical stealth techniques. Within a specific range, source interference and tin-strip interference can effectively conceal the aircraft in the interference crossed wave to make enemy's radar lose detection or tracking ability. Fig. 9 shows the changes in scattering power P_r, which is scattered back from an aircraft fuselage and received by a radar, and the interference power P_j received with the distance R between aircraft and radar when the radar is irradiating at the aircraft while the said aircraft is transmitting interference signals simultaneously. Since P_r is reversely proportional to R^4 and yet P_j is reversely proportional to R^2, the two curves intersect at one point under specific conditions. The distance R_{burn} corresponding to the intersecting point is called "burn-through distance". It can

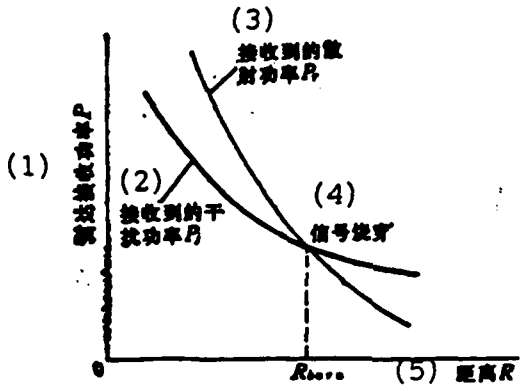

Fig. 9 Signal burn-through distance
Key: (1) Radar reception power P; (2) Interference power P_j received; (3) Scattering power P_r received (4) Signal burn-through; (5) Distance.

be seen from Fig. 9 that anuwhere within the range of $R>R_{burn}$, $P_j>P_r$ and the interference is successful; whereas within the range of $R<R_{burn}$, $P_r>P_j$ and the scattering signals of the aircraft can "pass-through" the interference signals and thus be detected. So, aircraft designer should find ways to reduce R_{burn} as much as possible in order to obtain sufficient concealed penetration distance. It is known from Reference [8] that

$$R_{burn}=\left[\frac{P_t G\cdot\sigma}{P_j G_j\cdot 4\pi}\right]^{\frac{1}{4}}* \qquad (1)$$

where P_t and P_j are radar and interference machine oupput power respectively;
G and G_j are radar and interference machine antenna power gain respectively;
σ is the radar scattering cross-section of aircraft along the direction of being irradiated.

It can be seen from equation (1) that there are two ways to increase stealth penetration distance (i.e. reduce R_{burn}); that is, reducing the radar scattering cross-section; increase the interference machine power. Before the advent of the

---

* The condition for using this equation is: aircraft with interference machine and radar are both at a high altitude quite distant from the ground (or sea surface), or the radar antenna employs a large angle of elevation to irradiate at the target. The equation is provided only for qualitative analysis purpose, and thus may not be restricted by this condition.

stealth airplanes (low radar scattering cross-section), Pj is increased solely by compressing R_{burn}, and thus increases in weight and volume of interference machine unacceptable to the aircraft designer are often resulted. Whereas now with the application of radar scattering cross-section reduction technique, this electronic interference technique which is difficult to continue to develop has found a new vitality. It may be seen from equation (1) that when σ is reduced by the tens and hundreds times, the interference machine power P_j required to guarantee the same R_{burn} will also be reduced by the tens and hundreds times.

It must also be noted that regardless of whether starting with reducing radar scattering cross-section of the aircraft or proceeding from increasing power of the interference machine in order to compress R_{burn} will invariably cause the expense of aircraft's full life period to rise and weight to increase. However, the magnitude of increase in weight caused by the two is different, and the increase in expense during the full life period occurs in different stages. Therefore, a full-scale weighing of the advantages and disadvantages is one task the designer of new aircraft can not ignore.

There also exists problems similar to those mentioned above between adopting tin-strip interference and radar bait devices and employing the radar scattering cross-section reduction technique. Therefore, in order to make an aircraft possess a specific stealth penetration ability the aircraft designer should derive reasonable answers from system analysis for the reduction indexes of radar scattering cross-section and the type, functions and power of electronic interference devices and specify them in the tactical technique requirements.

3. Tactical stealth techniques

Measures such as evading detection and tracking of enemy radar through appropriate flight cross-section designed for aircraft beforehand or self-adapting change of aircraft flight path during flight may be called the tactical stealth techniques. Sufficient attention should be given to cover the following three categories of tactical stealth technique in the tactical technique requirements.

(1) Conduct stealth penetration by taking advantage of the radar vision-distance blind region

The ability of radar wave diffracting along the earth curvature in general is relatively weaker, and therefore, if this kind of diffraction is omitted as an apporximate estimation, the fartherest distance a radar can see on the curved earth surface is limited by the "radar vision distance". The radar vision distance may be calcualted using the following formaula

$$R_h = \sqrt{2a_e}(\sqrt{h_a} + \sqrt{h_t}) \qquad (2)$$

where h_a and h_t are the radar antenna height and altitude of radar target respectively, and a_e=8493km which is the effective earth radius adopted for the consideration of atmospheric refraction.

Assume the height of a radar antenna, h_a=20m. For flying targets at different altitude h_t, the fartherest distance R_h capable of being detected by the said radar (assume it has sufficient irradiation power) is as shown in Table 3.

Table 3 Radar vision distance for target at different altitude

表3 目标在不同高度上的雷达视距

h_t(m)	20000	10000	1000	100	50	30	10	5	3
R_h(km)	601	431	149	60	48	41	31	28	26

Owing to the remarkable effects of this tactical stealth technique, currently the most advanced stealth airplanes and cruise missiles in foreigh countries also employ the super-low altitude penetration technique in addition to having an extremely low radar scattering cross-section. For this, they are all equipped with accurate terrain matching devices. The seatop flying altitude of some of the anti-ship guided missiles, such as the French "Exocet", can be maneuvered 3m to 7m based on difference in the height of sea surface. One of its purposes is also to compress the vision distance of enemy ship radar.

Currently the rise of radar with transcending vision distance (employing the reflection of the ionsphere to detect targets beyond vision distance), the application of airborn advance warning aircraft and the emergence of fighters with downward vision and firing ability have presented a great threat to minimum altitude flying. Judged by the entire air defense system, however, long-range penetration of aircraft must deal with the densely deployed and more numerous land-based radars along the seacoast and borders. Therefore, minimum altitude penetration will still

possess an important significance within a rather long period of time in the days to come. But there are different points of view in this respect which believe that entering the 21st century long-range combat airplanes will be forced to switch to maximum altitude penetration.

(2) Employing sea surface or ground surface crossed-wave interference to conduct minimum altitude penetration

If just the blind region of radar vision distance is employed to conduct stealth penetration, the aircraft is only able to get to 26km from the radar at most before it is exposed within the radar vision distance even if the flying altitude is lowered to 3m (see TAble 3). For short-range attack-type aircrafts such as anti-ship guided missile, 26km of exposed flight is more than adequate to make the anti-ship guided missile abort in the face of the ship's anti-missile system with a reaction time of less than 10 seconds. Therefore, this type of aircraft must still rely on sea surfave (or ground surface) crossed-wave interference to conduct stealth flight which will be able to get even closer to the radar. When an aircraft flies close to the ground surface or sea surface, as long as the wave petal of radar can irradiate at part of the aircraft and the ground surface (or sea surface) simultaneously, and the aircraft and the irradiated ground surface (or sea surface) are located at the same distanc from the radar antenna, then the signals received by the radar receiver will include crossed-wave type return wave of ground surface (or sea surface) in addition to the return wave of aircraft. Under normal conditions, the power of crossed-wave type return wave is much larger than the power of radar receiver noise. Useful signals from the target are interferred by this kind of crossed-wave signals thereby reducing radar's discovery probability. At this time, the factor that determines radar's discovery probability is no longer the signal/noise ratio, but the much smaller signal/crossed-wave ratio s/c:

$$s/c = \sigma_t F^4/\sigma^o R\theta_h(c\tau/2)\sec\psi \qquad (3)$$

where: σ_t is the radar scattering cross-section of target; F is the propagation factor of the radar antenna directional diagram which may be calculated using method in Chapter 6 of Reference [1]; R is the distance from the area center of

irradiated sea surface (or ground surface) to the radar antenna (i.e. distance from target to antenna); θ_h is the horizontal width of the radar wave petal (measures by rad); c is the propagation speed of electromagnetic wave; τ is the radar impulse width (measured by second); ψ is the angle between the ray aiming at the area center of irradiated surface and the irradiated surface generally referred as the "incident supplementary angle", and it may be obtained from geometric relations; σ° is the crossed-wave return wave coefficient and may be looked up from Reference [1] after the radar operating frequency, polarization pattern, sea surface conditions and incident supplementary angle are known.

After s/c is obtained from formula (3), the discovery probability P_d may be looked up from Fig. 11.2-4 in Reference [2] based on radar false alarm probability P_{fa} and impulse accumulation number N.

The smaller the s/c determined by formula (3) is, the smaller the aircraft's probability of being discovered, P_d, is. The only factor reflecting the flying altitude in formula (3) is the propagation factor F of the directional diagram, and within a sufficiently low altitude the lower the aircraft altitude is, the smaller F is and the smaller s/c is; and consequently the smaller the probability of being discovered is. Table 4 gives the calculated probability of being discovered of guided missiles such as the "Exocet" at different locations within sea surface crossed-wave interference region under the action of ship-carried low altitude searching radar SPS-39 (short-distance type). See Reference [5] for the primary parameters of SPS-39 (short-distance type) radar. The direct front radar scattering cross-section of guided missiles such as the "Exocet" is calculated based upon $0.1m^2$ under standard sea surface conditions: wave height $h_{1/3}$ = 1.2m and wind speed is 22 - 28km/hour. σ° in formula (3) takes the overall effects of tail winds, head winds and side winds into consideration.

It can be seen from Table 4 that the guided missile's probability of being discovered drops rapidly as the seatop altitude drops. When the seatop altitude drops to 3m, the probability of being discovered of guided missiles such as the "Exocet" can be smaller than 50%. It may be considered in a stealth penetration state at this time until penetrating to 6.1km from the target. Therefore, the seatop altitude of the "Exocet" is set at 3m-7m based on different sea surface conditions.

Table 4 Probability of being discovered, P_d, at different seatop altitudes for guided missiles such as the "Exocet"

(1)	导弹离雷达有限的距离(km)*	18.5	14	10	6.1
(2)	掠海高度10m P_d	96.2%	91.5%	83.5%	72%
(3)	掠海高度5m P_d	68%	24%	1.8%	81%
(4)	掠海高度3m P_d	46%	0.2%	5%	42%

*——也是导弹离雷达天线的距离。

Key: (1) Distance of guided missile from ship being attacked (km)*; (2) P_d at seatop altitude of 10m; (3) P_d at seatop altitude of 5m; (4) P_d at seatop altitude of 3m.
*---also the distance of guided missile from radar antenna.

Moving-target displaying radar presents a great threat to such stealth penetration as using the background crossed wave interference, for it is capable of separating moving targets from stationary backgrounds. This requires that the radar scattering cross-section of aircraft be further reduced by a large magnitude.

(3) Self-adapting evasion ability

The distribution of aircraft's radar scattering cross-section along different direction is extremely uneven. As shown in Fig. 7(a), if this aircraft employs a direction of ϕ=15° (or 345°) along an equi-directional angle curve to approach rather than using its direct front (ϕ=0°) to point at the enemy aircraft, then it basically employs a radar scattering cross-section of -8.7dBm² (i.e. 0.13m²) to aim at enemy aircraft's radar during the approach process instead of using the -3dBm² (i.e. 0.5m²) to point at the enemy aircraft's radar. 0.13m² is only 26% of 0.5m². In other words, the detection distance of enemy aircraft's radar can be compressed by 71%.

If an aircraft encounters the enemy aircraft while employing the intercrossing flight direction in the air and does not intend to engage in combat, then this aircraft had better avoid cutting across the irradiating direction of enemy aircraft's radar in a direction about ϕ=90° (or 270°). Because in this irradiation direction the radar scattering cross-section of aircrafts in general can be 20-30dB (100-1000 times) higher than those of the nearby directions.

Under this condition (take the aircraft in Fig. 7(a) as an example), the aircraft may use a directional angle of ϕ=45°-70° aimed at the irradiation direction of enemy aircraft's radar to perform a curved outflank maneuver, and then make a sudden, sharp turn while aiming at the irradiation direction of enemy aircraft's radar with a directional angle of ϕ=120°-140° to depart quickly. This measure is capable of evading the peak scattering cross-section of 16dBm^2 (i.e. 39.8m^2) while only exposing about -5dBm^2 (i.e. 0.32m^2), thereby reducing the action distance of enemy aircraft's radar by 30% and achieving the task of not being discovered by enemy aircraft.

In order to achieve the aforementioned self-adapting mobile maneuver for evading high scattering cross-section, the aircraft must be equipped with a set of electronic equipment which is capable of automatically detecting the irradiation direction and distance of enemy aircraft's radar, while making this set of equipment combine with the driving control system of the aircraft. Thus, the aircraft will obtain the self-adapting evasion ability, and generally this electronic equipment can be combined with the reconnaissance equipment in the interference system to form a complete set of device.

The three kinds of tactical stealth technique mentioned above can only be achieved through a set of advanced electronic equipment. The tactical stealth techniques employed, the technique indexes to be achieved and the corresponding electronic equipment should be clearly specified when the aircraft designer is drafting up the tactical technique requirements.

In conclusion, among the three categories which reflect the stealth penetration ability the ones that are most closely related to aircraft designer and are fundamentally significant are the scattering characteristics and radiation characteristics of aircraft, whereas the electronic interference ability and tactical stealth penetration ability are more related to the design and research of aeronautic electronic equipment.

This paper was reviewed by Professor Zhang Xichuen, and the auther hereby expresses his thanks.

REFERENCES

[1] Blake,V. Lamont.,Radar Range-Performance Analysis, (1980).

[2] DiFranco,J.V.and Rubin,W.L.,Radar Detection, (1968).

[3] 内藤一郎, 21世紀の軍用航空机を預測する, 第四回, 航空情報, (1982.10).

[4] 亘理昌晴, ステルス机に見る最新の電波 戦, 航空 情報, (1982,12).

[5] Norman Friedman, Naval Radar, (1981).

[6] アメリカ空軍机の最新極秘情報, 航空ファン (1983.2).

[7] Structural Concept and Aerodynamic Analysis for Low Radar Cross Section Fuselage Configurations, ADAO58906, july (1978).

[8] Radar Cross Section Fundamentles for Aircraft Designers, AIAA, 791818

[9] 資料！ナ B-1Bその総てを徹底解剖, 航空ジャーナル, (1982.2).

[10] Naval Radars in the Skimmer Age, *Defence Attache* No.2.(1983).

[11] 张考, 飞行器隐身技术国外发展概况, 雷达抗干扰论文选编, 电子对抗编辑部, (1986年4月)。

[12] 90年代の戦闘机の方向, 航空ジャーナル, (1985.7).

[13] New Air Force Fighter to Employ Stealth Design and Advanced Electronics,Defence Electronics April, (1984).

A Comprehensive Review of the Models for Predicting Fatigue Crack Growth Under Spectrum Loading

Si Erjian

Shanghai Aircraft Design and Reserach Institute

Submitted March 21, 1986

Abstract

This paper gives a comprehensive introduction and review of various models for predicting fatigue crack growth under spetrum loadings.

The basic principles, characteristic parameters, governing equations and strong and weak points of representative load interaction models presented by scholars both here and abroad in over ten years are tabulated for comparison. In addition, the selective principles, computation accuracy and cost-effectiveness of the models are discussed.

I. Forewords

In the design of damage tolerance for aircraft structure, the pattern of crack growth under complex spectrum loading must be first predicted whether estimating the structurla service life of determining maitenance cycle.

The loading an aircraft subject to is random, complex and constantly changing and the conditions under variable loading are much more complicated than constant loading. The interactions between loadings exert very grave influences on the rate of crack growth, and they primarily show up in:

(a) the slow down of rate of crack growth caused by tensile overloading, and it is generally called the "retardation effect".

(b) compression loading of the compression-tensile loadings cycle causing acceleration of crack growth, and this is called the "acceleration effect";

(c) compression loading of the compression-tensile loadings cycle causing the slow down of retardation effect caused by tensile overload , and this is called the "unloading effect".

The aforementioned effects are as shown in Fig. 1.

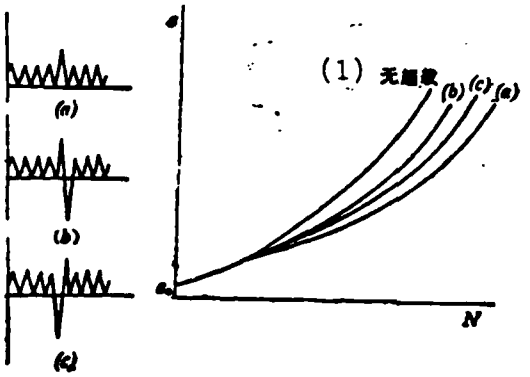

Fig. 1 Schematic of overload effects
Key: (1) No overload.

Ignoring the retardation effect of overloading will make life prediction too conservative, thereby causing increase in the weight of aircraft and economic losses. However, if the acceleration effect of compression loading and the delaying effect of compression loading on retardation are ignored, then it might make the design unsafe. Therefore, in the recent ten years people have given considerable attention to the computation of crack growth life under variable loadings and conducted a large quantity of research work and tests through which many models taking load interaction into account have been proposed. But since the elements of load interaction are extremely complex and many mechanisms are still unclear, various models often must rely upon specific tests and base on their respective assumptions, thus making them all have their own limitations.

THis paper conducts a comprehensive review of the representative load interaction models proposed in various countries in over ten years in order to seek effective and feasible methods for engineering applications.

II. Comparison of Various Models Taking Load Interaction Into Account

In early 70's, Wheeler[1], Willenborg[2] and Elber[3] proposed crack growth models taking overload retardation into account on after another.Numerous modified and new models have been developed on this basis. Now the more representative load interaction models from various countries are tabulated and compared. See Table 1.

Table 1 Comparison of Load Interaction Models

(1)模型名称	(2) 原 理 图	(3)模型的特征参数	(4) 裂 纹 的 计 算 公 式	(5) 优 缺 点
(1) Wheeler[1]	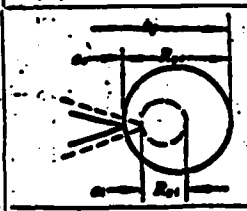	(6) 迟滞系数 $C_p=\left(\frac{R_{p1}}{a_p-a_1}\right)^m$	$\left(\frac{da}{dN}\right)_D=C_p\left(\frac{da}{dN}\right)_c=C_p\cdot C(\Delta K)^n$ $R_p=\frac{1}{a\pi}\left(\frac{K_{max}}{\sigma_y}\right)^2$, $\alpha=\begin{cases}2 & \text{平面应力}\\ 4\sqrt{3} & \text{平面应变}\end{cases}$ (7) (8)	(9)简便； (10)依据试验； (11)不能考虑的因素多。
(2) Willenborg[3]	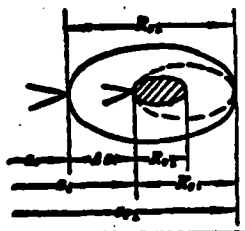	(12) 迟滞残余应力 $\sigma_{res}=\sigma_{max}-\sigma_{无延}$ (13)	$\frac{da}{dN}=f(\Delta K_{eff}, R_{eff})$ $\sigma_{max,eff}=\sigma_{max}-\sigma_{res}$ $\sigma_{无延}=\sigma_y\sqrt{\frac{a(a_{p1}-a_1)}{a_1}}$ $\alpha=\begin{cases}2 & \text{平面应力}\\ 6 & \text{平面应变}\end{cases}$ (7) (8)	(9)简便； (14)不需试验数据； (11)不能考虑的因素多； (15)结果偏危险。
(3) Elber[5]	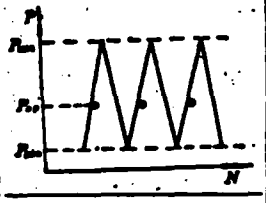	(16) 闭合参数 $U=\frac{\sigma_{max}-\sigma_{op}}{\sigma_{max}-\sigma_{min}}=\frac{\Delta\sigma_{eff}}{\Delta\sigma}$	$\frac{da}{dN}=c'(\Delta K_{eff})^{n'}=c'(U\Delta K)^{n'}$	(17)概念明确； (18)需试验确定张开应力。
(4) (19)中值法 Wheeler[6]	(20)同 (1)	(20)同 (1)	$\left(\frac{da}{dF}\right)_{n+1}=\left(\frac{\sigma_{max,eff}}{\sigma_{max,n}}\right)^{2m}\left(\frac{da}{dF}\right)_{1\sim n}$ (21) 或 $=\left(\frac{\sigma_{r,m,n}}{\sigma_{max}}\right)^{m}\left(\frac{da}{dF}\right)_{1\sim n}$	(20)同 (1)

(1) [illegible]	(2) [illegible]	(3) [illegible]	(4) [illegible]	(5) [illegible]
(5) (22) [illegible] Willenborg [6]	(20) [illegible] (3)	(23) [illegible] $\phi = \frac{1 - K_{max,th}/K^{w}_{max}}{S_{so} - 1}$	$\frac{da}{dN} = f(\Delta K_{eff}, R_{eff})$ $K_{max,min,eff} = K^{w}_{max,min} - \phi\left[K^{ol}_{max}\left(1 - \frac{\Delta a}{Z_{ol}}\right)^{+} - K^{w}_{max}\right]$	(9) [illegible]; (24) [illegible]
(6) ARFDL [8]	(25) 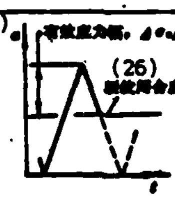	(27) [illegible] $C_f = \frac{\sigma_o}{\sigma_{max}}$	$\frac{da}{dN} = C\left[\frac{\sigma_{max}(1-C_f)}{1-C_{f0}}F(a)\right]^{n}$ $C_f = C_{f-1} + (C_{f0} - C_{f-1})(1+R)^{p}$ $\sigma_o = \sigma_{o1} - (\sigma_{o1} - \sigma_{o2})\left(\frac{\Delta a}{\rho}\right)^{B}$	(28) [illegible]; (29) [illegible]
(7) Maarse [7]	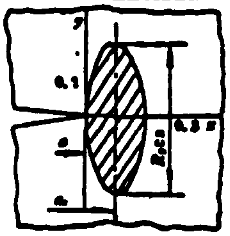	(30) [illegible] $P_{op} = \frac{\sigma_y B(\pi a)^{+}}{8(1-\nu^2)} \cdot \frac{R_{YCS}}{f\left(\frac{a}{W}\right)(a_0 - a)^{+}}$	$\frac{da}{dN} = C(U\Delta K)^{n}$ $U = \frac{P_{max} - P_{op}}{P_{max} - P_{min}}$ $R_{YCS} = 2w\left[\frac{1}{\pi}\left(\frac{K}{\sigma_y}\right)^2\right]$ $\left(\frac{X - 0.008}{0.008}\right)^2 + \left(\frac{Y}{0.234}\right)^2 = 1$ $x = a_0 - a$	(31) [illegible]; (28) [illegible]
(8) Matsuoka [8]	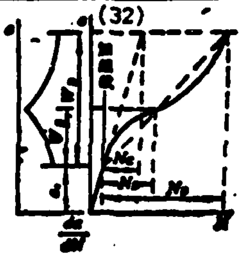	(6) [illegible] $U_D = \frac{\Delta\sigma_{eff}}{\Delta\sigma_2}$	$\left(\frac{da}{dN}\right)_D = C(U_D\Delta K)^{n}$ $U_D = \begin{cases} 1 - \left(\frac{\omega_B}{\omega_M}\right)^{+}(a - a_0)\left(\frac{1}{\omega_B} - \frac{1}{\omega_D}\right) & 0 \le a - a_0 \le \omega_B \\ 1 - \left(\frac{\omega_B}{\omega_M}\right)^{+}\left(1 - \frac{a - a_0}{\omega_D}\right) & \omega_B \le a - a_0 \le \omega_D \end{cases}$	(33) [illegible]; (28) [illegible]; (34) [illegible]

(1)[illegible]	(2)[illegible]	(3)[illegible]	(4)[illegible]	(5)[illegible]
(9) Willenborg/Chang[9]	图（3）	(35) [illegible]ϕ图(8)； (36) [illegible] $q=\left[\frac{\ln(r)}{\ln(1-R)}\right]/n$ (37) $(R<0)$ [illegible] $(Z_{ol})_{eff}$ $=(1+R_{eff})Z_{ol}$ $-1<R_{eff}<0$	$\frac{da}{dN}=\begin{cases}C[(1-R_{eff})^{m-1}(\Delta K)_{eff}]^n & R_{eff}>0 \\ C[(K_{max})_{eff}]^n & R_{eff}=0 \\ C[(1-R_{eff})^q(K_{max})_{eff}]^n & R_{eff}<0\end{cases}$ (39) (40) (38) $K_{max,eff}$ [illegible](8)	[illegible] [illegible]
(10) MPYZ[10]	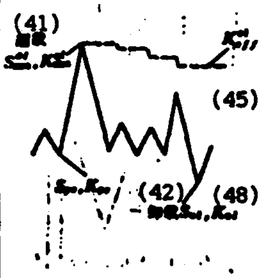 	(43) [illegible] $R_{eff}=\frac{K_{min}-K_R}{K_{max}-K_R}$ (44) [illegible] $K_R=\phi K_R^W$ (45) [illegible] (46) $\varphi=\frac{[illegible]B}{[illegible]\lambda}$ (47) (48) [illegible] $\beta=\frac{K_{pr}-K_{ol}}{K_{eff}^{ol}-K_{ol}}$	$\frac{da}{dN}=\frac{C(\Delta K)^n}{(1-R_{eff})^m K_c-\Delta K}$ (52) $m=\begin{cases}1 & R\geq 0 \\ 2 & R<0\end{cases}$ (53) $\phi=\begin{cases}\phi_R=\left[1-\frac{K_{th}}{K_{max}}\right]/[(\varphi-1)(1-R_l)] & \text{(49)} \Delta a+z_{op}<z_{ol} \\ \phi_A=1-R_l & \text{(50)} \Delta a+z_{op}>z_{ol}\end{cases}$ (54) $R_l=\frac{S_{ul}}{S_{max}^{ol}}$ (51) [illegible]，$K_{ol}=-\frac{K_{eff}^{ol}}{Z-Y}(Z-B)+K_{max}$	[illegible] [illegible] [illegible] [illegible]
(11) (55)[illegible][11]	(20)图（3）	(56) [illegible] $\sigma_{red}=\lambda\sigma_{1max}-\sigma_{2max}$ (16) [illegible] $U=\frac{1-\lambda(r-1)}{1-R_2}$	$\left(\frac{da}{dF}\right)_{var}=\left[\frac{1-\lambda(r-1)}{1-R_2}\right]^n\left(\frac{da}{dF}\right)_{linear}$ (57) (58) (59)	[illegible] [illegible] [illegible]

(1)[illegible]	(2)[illegible]	(3)[illegible]	(4)[illegible]	(5)[illegible]
(12) (60)[illegible][18]	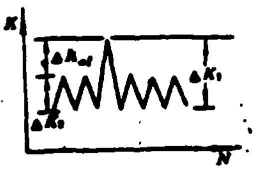	(61)[illegible] $(\sigma_e)_{min}$ $=a(\sigma_{eo}-\sigma_{Smax})$ (62)[illegible] $U=\frac{\Delta K_{eff}}{\Delta K_S}$	$\left(\frac{da}{dN}\right)=U\cdot\left(\frac{da}{dN}\right)_D$ (9) (63)[illegible]: $N_D=\frac{1}{\left(\frac{da}{dN}\right)_0}\int_0^{a_0}\frac{d\Delta a}{U_a}$ (59) $U=1+\frac{1-a}{1-R}-(1-a)\frac{K_{op}}{\Delta K_S}$ $1-a=\frac{1-\Delta K_{th}/\Delta K_S}{r_0-1}$	[illegible] [illegible]
(13) (64)[illegible][18] —Matsuishi[illegible] [illegible]	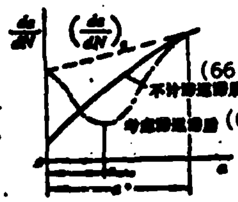	(68)[illegible] $a_{min}=120\frac{\sigma_{ys}}{E}R_y$	$\frac{da}{dN}=U_D\left(\frac{da}{dN}\right)_0$ (69) $U_D=\begin{cases}1-\left(\frac{r}{2}\right)\left(\frac{a^*}{a_{min}}-1\right)\frac{a}{a^*} & 0<a<a_{min}\\ 1-\left(\frac{r}{2}\right)\left(1-\frac{a}{a^*}\right) & a_{min}<a<a^*\end{cases}$ $a^*=\left[2.8\left(\frac{r}{2}\right)^2-\frac{1}{2}\left(\frac{1}{1-R}\right)^2\right]R_y^2$	[illegible]
(14) (70)[illegible][14] 1. (71)[illegible] Willenborg/Chang	(20)图(3)	(72)[illegible] $\alpha=\frac{6}{1+2S}$ $S=\frac{\Delta K-\Delta K_{th}}{(1-R)K_e}$	(73)同(8), [illegible] (76) $R_{eff}\geq 0$: (74) $Z_{el}=\frac{1}{\alpha\pi}\left(\frac{K_{max}}{\sigma_y}\right)^2$ (40) (74) $-1<R_{eff}<0$: $(Z_{el})_{eff}=(1+1R_{eff})Z_{el}$	[illegible] [illegible] [illegible]
2. (71)[illegible]	(20)图(7)		(75)同(7), [illegible] $\left(\frac{X-\frac{1}{2\alpha}}{\frac{1}{2\alpha}}\right)^2+\left(\frac{Y}{0.284}\right)^2=1$	

Key: (1) Model name; (2) Principle diagram; (3) Characteristic paramater of model; (4) Primary computation equation; (5) Strong and weak points; (6) Retardation coefficient; (7) Surface stress; (8) Surface strain; (9) Simple; (10) Rely upon tests; (11) Numerous factors not considered; (12) Retardation residual stress; (13) No retardation; (14) No test data required; (15) Results leaning toward danger; (16) Closure parameter; (17) Clear concept; (18) Tests Required to determine open stress; (19) Semi-linear; (20) Same as; (21) Or; (22) Generalized; (23) Proportional factor of residual stress; (24) Capable of taking factors such as threshold value of stress intensity factor and total retardation overload ratio, etc. into account; (25) Effective stress amplitude; (26) Crack closure stress; (27) Closure factor; (28) Numerous factors considered; (29) Heavy dependence upon tests; (30) Crack type open load; (31) Not relying upon tests; (32) Add overload; (33) More clear physical concept; (34) More difficult to apply to complex load spectrum; (35) Residual stress proportion factor ϕ same as; (36) Acceleration index; (37) Dimension of effective overload retardation region; (38) Expression same as; (39) Capable of taking the action of compression loading into account; (40) Convenient for engineering applications; (41) Overload; (42)Unload; (43) Effective stress ratio; (44) Residual stress intensity; (45) Overload effect coefficient; (46) End overload ratio (47) Non-retardation overload ratio; (48) Unload factor; (49) When...(retardation); (50) When...(acceleration); (51) When unloading; (52) Capable of taking factors such as unload effect, multi-overload action, etc. into account; (53) Simple equation, convenient for engineering applications; (54) Various parameters relying upon tests to be determined; (55) Huang Yuhuan model; (56) Residual stress; (57) Simple equation, quick computation; (58) Improve danger tendency of model; (59) Suitable for preliminary estimation when designing; (60) Ho Qingzhi model; (61) Minimum value of residual stress; (62) Effective coefficient of the amplitude value of stress intensity; (63) When yielding within small range; (64) Yang Bingxian model; (65) Improvement of; (66) Retardation delay not considered; (67) Retardation delay considered; (68) Minimum distance of overload retardation delay; (69) Capable of taking factors such as delay of retardation, etc. into account; (70) Yan Yuanzhang; (71) Modify; (72) Stress condition parameter; (73) Same as...where the modification of dimension of plastic region is; (74) When; (75) Same as...where the modification of ellipse equation is; (76) Capable of taking changes of stress conditions under spectrum loading.

III. Selection of Model Under Complex Spectrum Loading

The various models introduced by this paper are, based on their basic principles, classified into four major categories. The first category utilizes existing residual stresses at the tip of rear crack under the action of overload as the basis and employs the concept of effective stress intensity factor; the second category utilizes the crack close principle as the basis and employs the changes of crack open stress to study various influencing factors. The model expression of the first category is simpler, among which the Willenborg model at the beginning and later on the generalized Willenborg model have obtained extensive applications in the U.S. aerospace industry; its inadequacy, however, is its inability to take more influencing factors into account. The physical concepts of the second category

are clear, among which the Matsuoka model is capable of taking more factors into account; but these models contain more parameters and their applications have not been extensive.

In fact, it is difficult to build a model that includes every influencing factor and models too complex are often not very practical. Some of the models which are capable of grasping the main contradictions have been able to, within a specific range, obtain more satisfactory results. Therefore, aiming at research subjects and selecting suitable models is the first major step in the work of predicting crack growth life.

1. Selection principle of model

The selection principle of models under complex spectrum loading can be classified into the following three items: first, the model must be able to take overload delay, compression loading and its coupling effect into account; second, the model should utilize linear elastic fracture mechanics (LEFM) as the basis, i.e. the crack growth phenomenon should regard stress intensity factor range ΔK as the characteristic amount; third, the model should utilize test data of crack growth under equi-amplitude loading and avoid lengthy computation as much as possible in order to allow for convenient engineering applications.

2. Computation accuracy and cost-effectiveness

In can be seen from the comparison in Table 1 that various models have their own specific range. Selecting reasonable model aiming at specific conditions is the chief prerequisite for obtaining computation accuracy. In addition, the cumulative computation method for crack growth also directly affects computation accuracy. There are numerous numerical computation methods for crack growth and due to limitations on space, they will not be discussed in this paper. Only a brief introduction of the comparison between computation results of several models and tests is made here, see Table 2 (selected from References [9], [10] and [14]).

It can be seen from Table 2 that the computation results of model (5) tend to be unsafe because the effects of negative loading are not considered, whereas the computation accuracy has been improved for several other models which take the effects of negative loading into consideration.

Table 2 Comparison of tests and analyses of crack growth under spectrum loading

(1) 试件号	(2) 载荷谱类型 (6)	(3) 试验寿命 N_T(cycles)	(4) 分析估算寿命 N_p, (cycles) (5) 模型(5)	$\left(\frac{N_p-N_T}{N_T}\right)$ (5) 模型(9)	(5) 模型(10)	(5) 模型(14)
M-81	战斗机 A-A	115700	213110 (0.84)	168720 (0.46)	137000 (0.18)	167985 (0.45)
M-82 (6)	战斗机 A-A	58585	74055 (0.26)	53312 (-0.09)	57000 (-0.03)	53997 (-0.08)
⋮						
M-85 (6)	战斗机 A-G	95842	131868 (0.38)	91816 (-0.04)	90020 (-0.06)	91961 (-0.04)
⋮						
M-84 (7)	运输机混合谱	279000	628074 (1.25)	318060 (0.14)	257000 (-0.08)	—
$\left(\frac{N_p-N_T}{N_T}\right)$ (8) 平均			(0.74)*	(0.13)*	(0.11)*	(0.08)**
(9) 标准差			(0.42)	(0.22)	(0.20)	

(10)* 为13个试验件的平均值
(11)** 为6个试验件的平均值

Key: (1) Test item number; ~~(2) Type of spectrum~~ loading; (3) Test life; (4) Analytical estimated life; (5) Model; (6) Fighter; (7) Cargo plane mixed spectrum; (8) Average; (9) Standard deviation; (10) Average value of 13 test items; (11) Average value of 6 test items.

Certainly, obtaining computation accuracy is often contradictory to cost and this requires that a choice be made between the demands of the two. Take simple spectrum (e.g. the not nonobvious ground-air-ground cycle) or random spectrum for example, sometimes using the linear culmulative method or the root mean square method which do not take the effects of loading sequence into account can not only obtain better computation results but also save computer time; whereas for complex spectrum with greater changes in spectrum type, the effects of loading sequence must be considered.

IV. Conclusions

Based on the aforementioned model selection principle, the author believes that the improved generalized Willenborg model, i.e. the Willenborg/Chang model

not only takes various effects into account but also allow for convenient applications which provides an effective method for engineering. In general, those models which were proposed by scholars of our country and introduced in this paper have all made reasonable improvements on the basis of models proposed by their predecessors. These models are simple, do not require large amount of test sata, easy to use and have better practical values.

Presently, the idea of damage tolerance design is developing rapidly in our country and the analysis of crack growth under spectrum loading is one of the important contents of damage tolerance design. Judged from the needs of engineering practices, furhter understanding the mechanisms of load interaction through tests and studies in order to search for crack growth models that are high performance and convenient to applications is a task worth paying attention to.

REFERENCES

[1] Wheeler, O.E., Spectrum Loading and Crack Growth, ASME, D, Vol. 94, No. 1, (1972).

[2] Willenborg, T.D., Engle, R.M. and Wood, H. A., A Crack Growth Retardation Model Using an Effective Stress Concept, AFFDL-TM-71-1-FBR, (1971).

[3] Elber, W., The Significance of Fatigue Crack Closure, ASTM STP 486, (1971).

[4] Brock, D., Spectrum Loading Fatigue Crack-Growth Prediction and Safety Factor Analysis, AD A061920, (1976).

[5] Gallagher, J.P., A Generalized Development of Yield Zone models, AFFDL-TM-74-28-FBR, (1974).

[6] Bell, P.D. and Creager, M., Crack Growth Analysis for Arbitrary Spectrum Loading, AFFDL-TR-74-129, (1974).

[7] Maerre, J., Crack Closure Related to Fatigue Crack Propagation, ICF4, Vol. 2B, (1977).

[8] Matsuoka, S., Tanaka, K. and Kawahara, M., The Retardation Phenomenon of Fatigue Crack Growth in HT80 Steel, Eng. Fract. Mech, Vol. 18, No. 3, (1976).

[9] Chang, J.B., Engle, R.M. and Szamossi, M., An Improved Methodology for Predicting Random Spectrum Load Interaction Effects on Fatigue Crack Growth, ICF5, Vol. 5, (1981).

[10] Johnson, W.S., Multi-Parameter Yield Zone Model for Predicting Spetrum crack Growth, ASTM STP 748, (1981).

[11] 黄玉瑚，刘雪嘉，单线性Willenborg迟滞模型，西北工业大学科技资料SHj8003,(1980)。

[12] 何庆芝，考虑过载迟滞效应的一个新模型，北京航空学院学报，No.1,(1980)。

[13] 杨荣宪，谐载荷作用下裂纹延长模型，北京航空学院学报，No.3,(1981)。

[14] 张永存，顾明达，顾鸣泉，谐载荷下裂纹扩展计算模型及其在民实飞行谱中的应用，航空材料第2卷第2期，(1982)。

DISTRIBUTION LIST

DISTRIBUTION DIRECT TO RECIPIENT

ORGANIZATION	MICROFICHE
A205 DMAHTC	1
A210 DMAAC	1
B344 DIA/RTS-2C	9
C043 USAMIIA	1
C500 TRADOC	1
C509 BALLISTIC RES LAB	1
C510 R&T LABS/AVRADCOM	1
C513 ARRADCOM	1
C535 AVRADCOM/TSARCOM	1
C539 TRASANA	1
C591 FSTC	4
C619 MIA REDSTONE	1
D008 NISC	1
E053 HQ USAF/INET	1
E404 AEDC/DOF	1
E408 AFWL	1
E410 AD/IND	1
E429 SD/IND	1
P005 DOE/ISA/DDI	1
P050 CIA/OCR/ADD/SD	2
AFIT/LDE	1
FTD	
CCN	1
NIA/PHS	1
LLNL/Code L-389	1
NASA/NST-44	1
NSA/T513/TDL	2
ASD/FTD/NIA	1
FSL/NIX-3	1

END

DATE

FILMED

9-88

DTIC